Progress In Electromagnetics Research C, Vol. 117, 261–276, 2021

Modified Spokes Wheel Shaped MIMO Antenna System for Multiband and Future 5G Applications: Design and Measurement

Sumeet S. Bhatia[1, *] and Narinder Sharma[2]

Abstract—In this manuscript, a modified spokes wheel shaped two port MIMO (Multi-Input-Multi-Output) antenna with stub loaded ground plane has been presented and experimentally analysed for multiband and EU (European Union) 5900 to 6400 MHz for future 5G mobile terminal applications. The proposed MIMO antenna consists of two radiating patches, and its ground plane is modified to achieve the multiband characteristics as well as enhanced isolation. Initially, a rectangular notch, at the center of ground plane (Ground-1), is employed and reveals four resonant points. Further, the ground plane is modified again by employing two inverted L-shaped stubs along with a series of horizontal rectangular stubs (Ground-2) for enhancing the isolation and reducing the mutual coupling between the elements of proposed MIMO antenna. The antenna with ground-2 exhibits seven frequency bands ($S_{11} \leq -10$ dB) 2.2, 6.0, 7.9, 9.6, 11.1, 12.7, and 15.6 GHz with corresponding isolation ($S_{12/21}$) −19.47, −31.22, −34.63, −30.05, −27.16, −39.08, and −22.28 dB. Diversity performance parameters of the proposed MIMO antenna such as ECC, DG, CCL, TARC, and MEG are in acceptable limits at each operational frequency band. The proposed MIMO antenna is designed and fabricated on a low cost FR4 glass epoxy substrate, and the simulations are carried out by using FEM based Ansys HFSS V13 simulator. Simulated and measured results are compared and found in good agreement with each other.

1. INTRODUCTION

In the present era of technology, there is an increasing demand of portable/hand-held wireless devices, which should be proficient to transfer or receive the audio/video streaming with high data transfer rate and good transmission quality. A large channel capacity is required to transmit these messages at high data rate without signal quality loss. According to the Shannon's theorem, a conventional single-input, single-output (SISO) communication system is incapable of these operations because of its limited channel capacity. Distinct techniques and approaches have been employed by researchers to overcome this problem. After various attempts to resolve the said problem, Multiple-input Multiple-output (MIMO) communication system came into existence which is capable to transfer the data with high rate and reduce the signal fading in a rich scattering environment without any extra expenditure in power or spectrum. Antennas used in such communication systems are said to be MIMO antennas which are capable of inherently mitigating the effects of multipath, network throughput, causing a better-quality link reliability, gain, channel capacity, coverage without requiring additional bandwidth, and diversity performance because of spatial (or signalling) degree of freedom that is absent in SISO systems. Space Time Coding (STC) and Spatial Multiplexing techniques are also employed in MIMO systems to attain lossless faster data rate. STC helps to achieve the diversity, and Spatial Multiplexing enables a MIMO transmitter/receiver pair to increase its throughput without increasing transmission power or bandwidth

Received 11 November 2021, Accepted 6 January 2022, Scheduled 10 January 2022

* Corresponding author: Sumeet Singh Bhatia (sumeet.bhatia8@gmail.com).

[1] Electronics and Communication Engineering Department, Yadavindra College of Engineering and Technology, Guru Kashi Campus, Punjabi University, Talwandi Sabo, Bathinda, Punjab, India. [2] Dean Research and Development, Amritsar Group of Colleges, Amritsar, Punjab 143001, India.

usage. Printed monopole antennas are extensively used in the MIMO systems for their advantages of less cost, ease of fabrication, and good performance. MIMO antenna usually comprises at least two radiating elements, placed at some definite distance with high isolation between them. The available space is very limited in the hand-held/portable wireless front-ends which may result in mutual coupling and distort the performance. To reduce mutual coupling and increase isolation, without compromising the performance, various techniques and methods have been suggested by scientists. Chung et al. [1] have designed a multiband MIMO antenna for mobile application. This paper presents an antenna which operates in the frequency range of 2.3–2.69 GHz and WCDMA applications. A novel design of a MIMO antenna has been designed by Sehrai et al. [2] for 5G milli-meter wave applications with high gain wideband applications. Yang et al. [3] have illustrated a multiband MIMO antenna for different wireless standards such as GSM, DCS, and LTE indoor applications. The designed antenna in this manuscript has been fed by a 50 Ω CPW transmission line to generate proper impedance matching characteristics. Hatte and Patil [4] have explained the design methods of MIMO antenna for 5G mobile terminal applications. This review article reveals the detailed study of 5G communication technology for the leading telecommunication companies of the world. A compact dual band two element MIMO antenna has been designed by Nandi and Mohan [5] for WLAN applications. In this antenna, two quarter wavelength slots have been used which radiates at 2.5 and 5.6 GHz frequency bands. Similarly, a dual band MIMO antenna has been designed by Huang et al. [6] for 5G and WLAN mobile terminal applications. This antenna is composed of an open-loop ring resonator feeding element and a T-shaped radiating element. Deng et al. [7] have designed a dual-band MIMO antenna using meandering line resonating elements for WLAN applications. The antenna designed in this article operates in 2.4–2.48 GHz and 5.15–5.825 GHz frequency ranges. Also, a triple-band MIMO antenna has been designed for 5G applications by Kumar et al. [8]. In this paper, authors have used two concentric circular slot ring radiators etched on the ground plane of the antenna for each radiating element. Likewise, a dual-band planar MIMO antenna is illustrated by Liu et al. [9] for WLAN frequency band applications. Ishteyaq and Muzaffar [10] give an in-depth explanation and review on the evolution of the 5G spectrum allocation along with the characteristics of MIMO antenna. This article also explains the MIMO antenna design in regards to the reduction in mutual coupling and safer user applications. Talha et al. [11] illustrated the design of a compact MIMO antenna system which operates in the frequency range from 5 to 7.3 GHz with reduced mutual coupling. Wang et al. [12] have designed a millimetre-wave wideband MIMO antenna for 5G communication applications with high isolation. This antenna operates in the frequency range from 24 to 39 GHz which can easily covers most of the applications in the Ka band. A compact dual-band antenna has been designed by Nirmal et al. [13] with improved isolation for wireless applications such as Wi-MAX and WLAN which operates in the frequency bands of 3.5 and 5.8 GHz, respectively. Iqbal et al. [14] have used F-shaped stubs in shared ground plane to reduce the mutual coupling in UWB-MIMO antenna design. Sun et al. [15] have designed a triple-band MIMO antenna by using a meander-line inverted L-shaped radiator for mobile wireless applications such as GSM900/1800 and LTE2600. Similarly, a MIMO antenna for GSM and LTE applications has been designed by Asadpor and Rezvani [16]. This antenna is designed by using folded microstrip line fed and L-shaped slots which are connected with an isolation line to reduce the coupling effect between the ports. Also, CSRRs are used to enhance the isolation as well as to control the resonant frequencies. Deng et al. [17] have designed a dual-band inverted-F MIMO antenna for WLAN applications with enhanced isolation. Also, a decoupled multiband MIMO antenna has been illustrated by Dong et al. [18] for WWAN/LTE smartphone applications. This MIMO antenna system is composed of two groups of symmetrical bending structures and uses the structure of slotted and protruded ground to reduce the coupling between elements. Khan et al. [19] have designed a dual band MIMO dielectric resonator antenna for WLAN (5.15–5.35 GHz) and WiMAX (3.4–3.7 GHz) applications. This antenna exhibits the impedance bandwidth of 9.97% at 3.6 GHz and 8.88% at 5.2 GHz frequency band. Wang et al. [20] have designed a MIMO antenna system which operates in the wideband frequency range from 3300 to 6400 MHz for future 5G mobile terminal applications.

By thoroughly reviewing the aforementioned literature, the authors have designed a novel modified spokes wheel shaped MIMO antenna for multiband and future 5G applications. The proposed MIMO antenna consists of two radiating patches, and its ground plane is modified to achieve multiband characteristics with high isolation characteristics.

The rest of the paper is organized as follows. Section 2 presents the design of the MIMO antenna with its fabricated structure and evolution of the proposed antenna along with the various simulated results and variation graphs of different optimized parameters of antenna. Section 3 demonstrates the experimental results and discussion of various S-parameters of proposed MIMO antenna. Section 4 reveals the comparison of simulated and measured diversity performance parameters along with detailed explanation, followed by conclusion.

2. ANTENNA DESIGN

2.1. Antenna Configuration

The structure of proposed multiband modified spokes wheel (MSW) shaped two port MIMO antenna with stub loaded ground plane is shown in Fig. 1. The overall dimensions of designed antenna are $30 \times 52 \times 1.6\,\text{mm}^3$. It consists of two indistinguishable modified spokes wheel shaped radiating elements. Fractional ground plane with two Inverted L-shaped stubs along with a series of horizontal rectangular stubs are employed to improve the isolation. The proposed antenna is fabricated on an abundantly available low cost FR4 glass epoxy substrate with height = 1.6 mm, dielectric constant = 4.4, mass density = $19,000\,\text{kg/m}^3$, and loss tangent = 0.02; and its fabricated prototype is delineated in Fig. 2. The optimized parametric dimensions of the proposed two port MIMO antenna are tabulated in Table 1 for more lucidity.

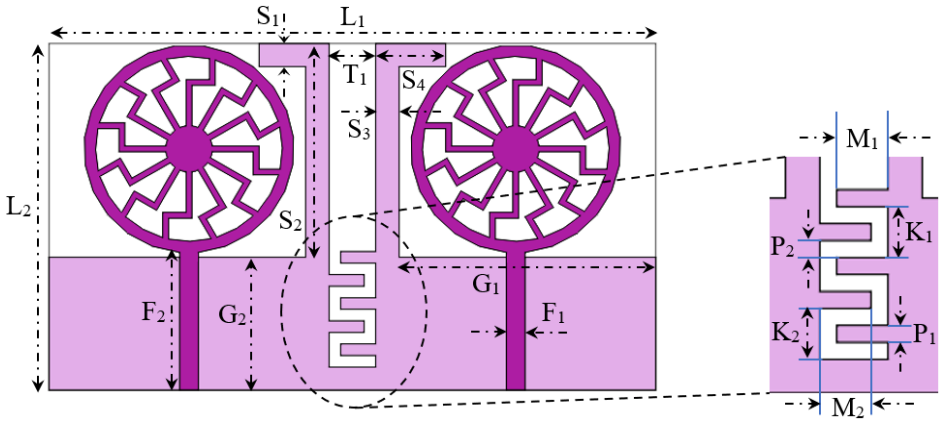

Figure 1. Geometrical structure of proposed MSW shaped two port MIMO antenna.

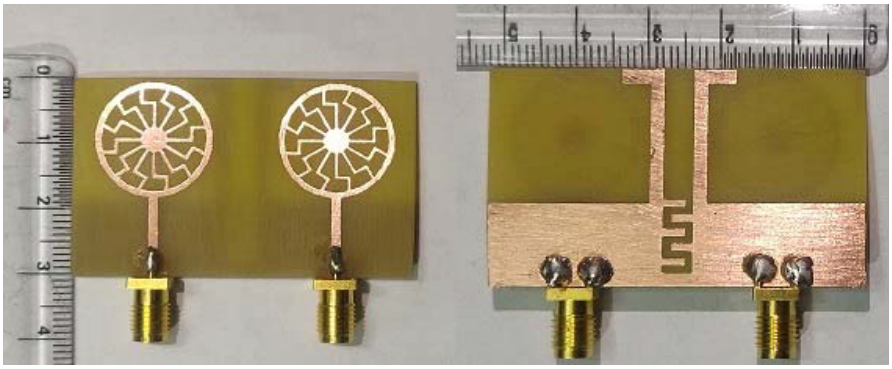

Figure 2. Fabricated prototype of front and back view of proposed MSW shaped two port MIMO antenna.

Table 1. Optimized parametric dimensions of proposed MSW shaped MIMO antenna (unit in mm).

L_1	L_2	F_1	F_2	S_1	S_2	S_3	S_4	G_1	G_2	T_1	M_1
52	30	1.6	11.9	2.0	18.5	2.0	6.0	22	11.5	4	3.0
M_2	P_1	P_2	K_1	K_2	R_1	R_2	R_3	Y_1	Y_2	Y_3	Y_4
3.0	1.0	1.0	3.0	3.0	9.0	8.0	2.0	2.0	2.3	4.0	0.5

2.2. Effects and Designing of Single Antenna Unit

Initially, the single unit of proposed antenna has a circle-shaped radiating patch whose outer radius 'R_1' has been evaluated by using the following equations [21, 22], and the circular geometry with radius 'R_2' is etched from the patch to generate the desired ring-shaped structure and acts as an outer surface of the wheel as illustrated in Fig. 3(a). Further, the modified spoke, portrayed in Fig. 3(b) has been attached to the ring-shaped patch at an angle of 30° from the centre along with the circular element of radius 'R_3' concentric to the circular ring in order to obtain the MSW shaped geometry of radiating patch as shown in Fig. 3(c). To analyse the effects of different structures of radiating patch, the 50 Ω transmission line feed has been used along with the fractional ground plane. All the designed structures of antenna have been simulated by using finite element method (FEM) based HFSS V13 simulator. The different evolution steps for the designing of single unit of proposed MIMO antenna are reported in Fig. 4, and the comparison of reflection coefficient curves of the steps is envisaged in Fig. 5.

$$R_1 = \frac{F}{\left\{1 + \frac{2h}{\pi F \varepsilon_r}\left[\ln\left(\frac{\pi F}{2h}\right) + 1.7726\right]\right\}^{\frac{1}{2}}} \tag{1}$$

where,

$$F = \frac{8.791 \times 10^9}{f_r\sqrt{\varepsilon_r}} \tag{2}$$

It can be contemplated from Fig. 5 that the antenna designed in Step-1 (containing four spokes) exhibits quad frequency points at 6.6, 8.8, 13.1, and 15.4 GHz with impedance bandwidths of 4.36 GHz (5.32–9.68 GHz) and 4.68 GHz (11.68–16.36 GHz). Further, by increasing the number of spokes (eight spokes) in the wheel shaped radiating patch as shown in Fig. 4(b), the antenna resonates at five frequency bands with initial resonant point 6.6 GHz similar to previous step. Step-2 antenna reveals the bandwidths of 4.39 GHz (5.1–9.49 GHz), 1.11 GHz (9.92–11.03 GHz), and 4.46 GHz (12.47–16.93 GHz). Likewise, by applying the four more spokes in the previous geometry (Step-2), the final structure of MSW shaped patch (Step-3) is generated and depicted in Fig. 4(c). This geometry exhibits one more frequency band

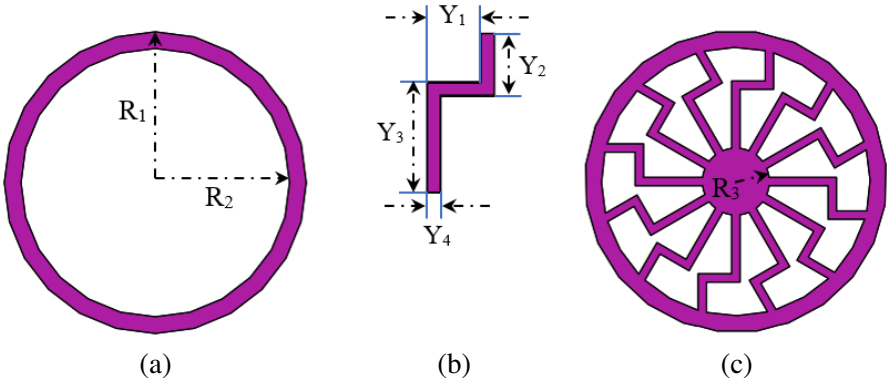

Figure 3. Steps for designing the proposed structure of radiating patch; (a) circular ring-shape, (b) modified spoke and (c) MSW shaped radiating patch.

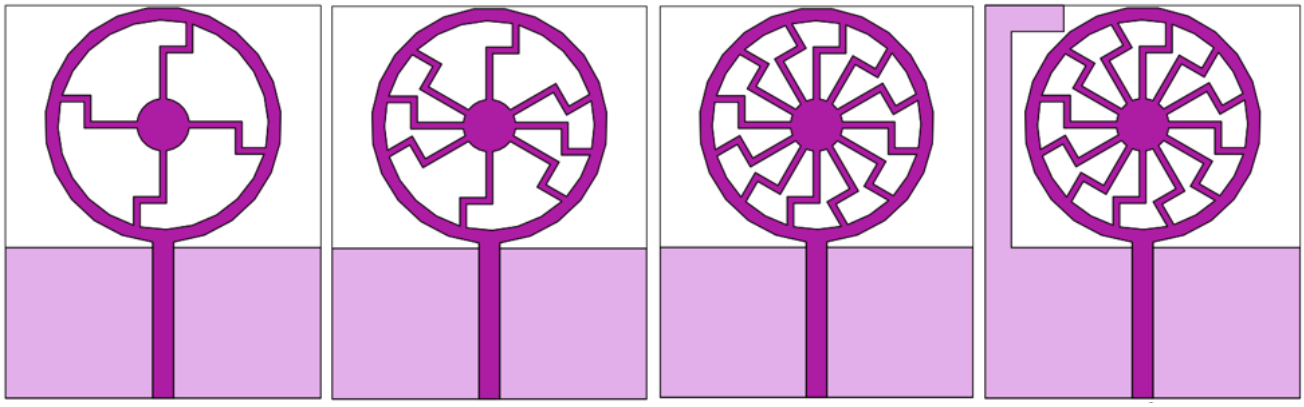

Figure 4. Evolution steps for the designing of single unit of proposed MIMO antenna: (a) Step-1, (b) Step-2, (c) Step-3 and (d) Step-4 (proposed single unit).

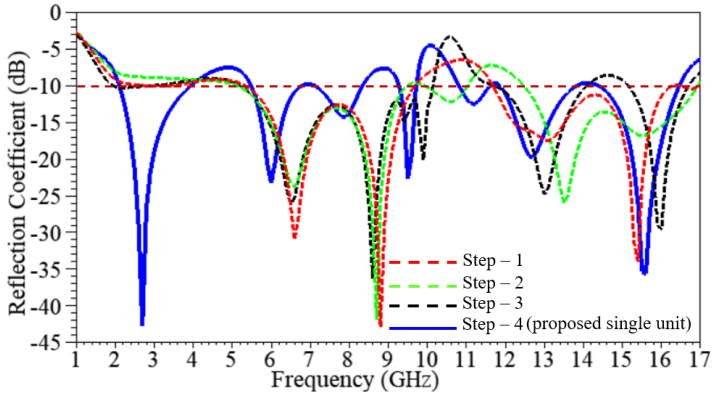

Figure 5. Comparison of reflection coefficient versus frequency plot of different steps of single antenna unit of proposed MIMO antenna.

and resonates at six unique frequencies (6.6, 8.6, 9.4, 9.9, 13.0, and 16.0 GHz) as compared to Step-1 and Step-2 and also reports improved impedance bandwidth of 4.95 GHz (5.2–10.15 GHz) at lower frequency bands. From, above discussion, it can be predicted that by increasing the count of spokes in the different designing steps of single unit of the proposed antenna, the number of frequency bands also gets increased with enhanced bandwidth.

To improve the performance of the antenna designed in Step-3, a new antenna (Step-4) has been created by applying an inverted L-shaped stub in fractional ground plane as delineated in Fig. 4(d), and its corresponding reflection coefficient curve is shown in Fig. 5 (royal blue solid line). It can be anticipated from Fig. 5 that the antenna designed in Step-4 helps in obtaining additional frequency band at 2.7 GHz along with the other six frequency bands, as well as shifting frequency band from 6.6 GHz to 6.0 GHz. It is worth noted that the resonant frequency band at 6.0 GHz is closer to the resonant frequency band obtained by using afore-said calculations and clearly satisfies Equations (3) and (4). Miniaturization (reducing the overall size of antenna) has been attained due to the exhibition of additional frequency band at lower side along with the frequency shift. Thus, it is evident from these results that the antenna structure designed in Step-4 acts as a final geometry of single element of proposed MSW shaped two port MIMO antenna due to the enhanced performance parameters in terms of impedance characteristics with increased number of frequency bands. The performance of proposed MIMO antenna will be discussed in detail in upcoming subsections.

2.3. Effects of Ground Plane on Proposed Two Port MIMO Antenna

The evolution stages of ground plane (Ground-1 and 2) for the proposed MSW shaped MIMO antenna are delineated in Fig. 6. Simulated S-parameters of MIMO antenna for both the configurations of ground plane are illustrated in Figs. 7 and 8, respectively. S_{11} and S_{21} are almost identical to S_{22} and S_{12} because of symmetrical antenna elements. Hence, only S_{11} and S_{21} are shown in Figs. 7 and 8.

Figure 6. Evolution stages of the ground plane of proposed MIMO antenna.

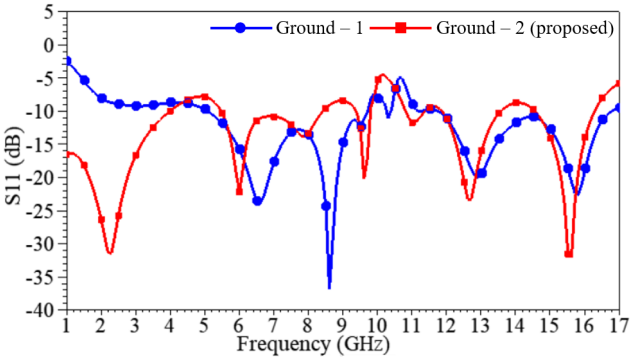

Figure 7. S_{11} parameter of MSW shaped MIMO antenna for different configuration of ground plane.

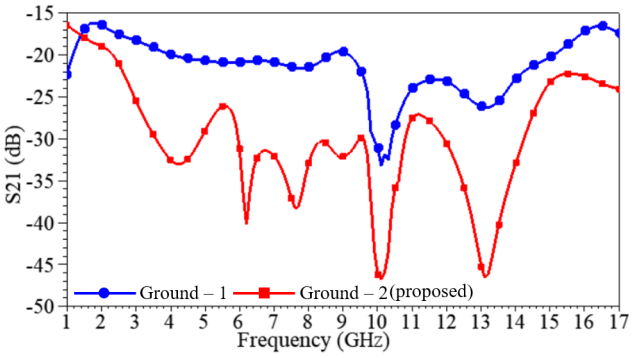

Figure 8. S_{21} parameter of MSW shaped MIMO antenna for different configuration of ground plane.

The MIMO antenna with Ground-1 exhibits dual frequency ranges from 5.05 to 9.97 GHz and 11.42 to 16.56 GHz (for $S_{11} < -10$ dB) with mutual coupling (S_{21}) below -20 dB in the frequency range of 5.05–9.20 GHz and -20 to -30 dB in the frequency range 9.21–9.97 GHz. Similarly, the mutual coupling S_{21} is between -20 and -25 dB in the frequency range from 11.42 to 15.10 GHz and -16 to -20 dB in frequency range 15.11 to 16.56 GHz. From above discussion, it is evident that the antenna with Ground-1 is useful for MIMO operation due to the mutual coupling below -15 dB in the afore-said frequency ranges. This MIMO antenna (with Ground-1) also portrays quad frequency bands 6.6, 8.6, 12.9, and 15.8 GHz in the operational frequency ranges.

However, to further reduce the mutual coupling and increase the number of frequency bands, Ground-2 is designed and introduced in the geometry of proposed MIMO antenna. Ground-2 consists of two inverted L-shaped stubs along with a series of horizontal rectangular stubs as limned in Fig. 6. After employing Ground-2, it can be contemplated that lower cut-off frequency has been shifted from 5.05 GHz to 1.0 GHz and also exhibited the mutual coupling of -16 to -25 dB in the frequency range from 1.0 to 2.95 GHz; below -25 dB in the frequency range 2.96 to 14.7 GHz and -20 dB in the rest of frequency range up to 17 GHz. The proposed antenna embellish seven unique frequency bands at 2.2, 6.0, 7.9, 9.6, 11.1, 12.7, and 15.6 GHz with corresponding reduced mutual coupling (S_{21}) -19.47, -31.22,

−34.63, −30.05, −27.16, −39.08, and −22.28 dB, respectively. MIMO antenna with Ground-2 can be said as a proficient candidate for applications in the frequency ranges of 1.0–4.0 GHz, 5.47–8.41 GHz, 9.36–9.79 GHz, 10.80–11.38 GHz, 11.86–13.56 GHz, and 14.54–16.27 GHz. It can be anticipated from above discussion that ground plane plays a pivotal role in the improvement of performance parameters of proposed MIMO antenna in terms of isolation and number of frequency bands. Miniaturization is also attained because frequency is shifted from 5.05 to 1.0 GHz. The comparison of the results of proposed MIMO geometries of antenna with different ground configurations are tabulated in Table 2, for better understanding.

Table 2. Comparison of results for proposed MIMO geometries of antenna with different ground configuration.

Proposed MIMO antenna design	Resonant frequency bands (GHz)	(F_L) Lower frequency (GHz)	(F_L) Lower frequency (GHz)	S_{11}/S_{22} (dB)	S_{21}/S_{12} (dB)	Bandwidth (GHz)
Ground-1	6.6	5.05		−23.97	−20.75	4.92
	8.6		9.97	−36.77	−20.09	
	12.9	11.42		−20.02	−26.02	5.14
	15.8		16.56	−22.62	−17.82	
Ground-2 (proposed antenna)	2.2	1.00	4.00	−31.37	−19.47	3.00
	6.0	5.47		−22.20	−31.22	2.94
	7.9		8.41	−13.82	−34.36	
	9.6	9.36	9.79	−20.24	−30.05	0.43
	11.1	10.80	11.38	−11.68	−27.16	0.58
	12.7	11.86	13.56	−23.30	−39.08	1.70
	15.6	14.54	16.27	−32.12	−22.28	1.73

The effects of different ground plane configurations on surface current distributions at 2.2, 6.0, and 9.6 GHz frequency are shown in Fig. 9. In the two-port MIMO antenna, one port is excited, while the other port is terminated with a matched load of 50 Ω. Thus, port-1 and port-2 of the proposed MIMO antenna are excited and terminated with 50 Ω load respectively as delineated in Fig. 9. It can be clearly understood from Fig. 9 that more current is coupled towards inverted L-shaped stubs along with a series of horizontal rectangular stubs and transmission line feed. At the moment, surface current comes closer to another monopole element, and it will get reduced. It undoubtedly specifies the reduction of mutual coupling between the ports.

3. RESULTS AND DISCUSSION

The modified spokes wheel (MSW) shaped two port MIMO antenna has been fabricated, and the results of the fabricated MIMO antenna are juxtaposed to corroborate the simulated results. The prototype of antenna is shown in Fig. 2, and its results are measured using Vector Network Analyzer (VNA).

The comparison between experimental and simulated S-parameters is illustrated in Figs. 10 and 11. Small discrepancy has been noted between the simulated and measured results which may have occured due to the fabrication weaknesses such as connector soldering bumps, improper copper etching, and some alterations in physical dimensions of the fabricated prototype. It can be observed from Fig. 10 that measured reflection coefficient is below −10 dB for the operational frequency bands 2.2, 6.0, 7.9, 9.6, 11.1, 12.7, and 15.6 GHz. It can be anticipated from Fig. 11 that the isolation of measured MIMO antenna is

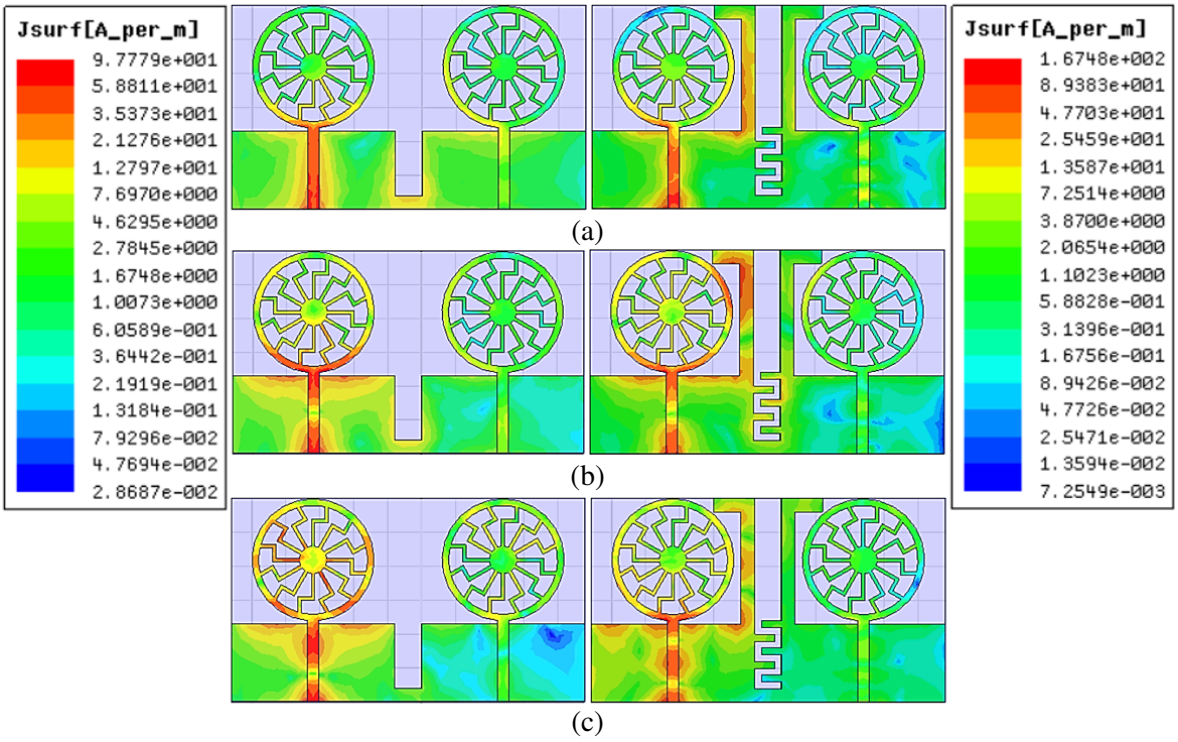

Figure 9. Surface current distribution of proposed MIMO antenna by making port-1 excited and port-2 terminated at (a) 2.2, (b) 6.0 and (c) 9.6 GHz.

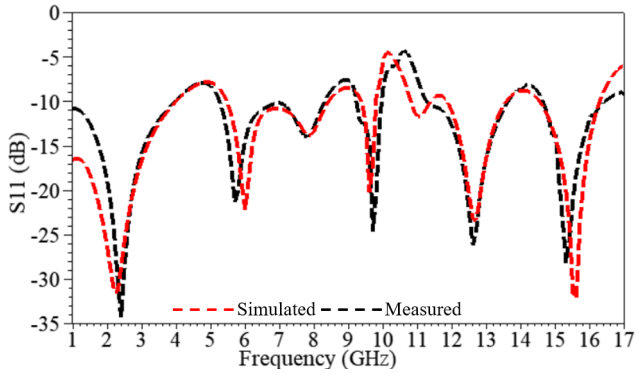

Figure 10. Comparison of S_{11} parameter of proposed MIMO antenna.

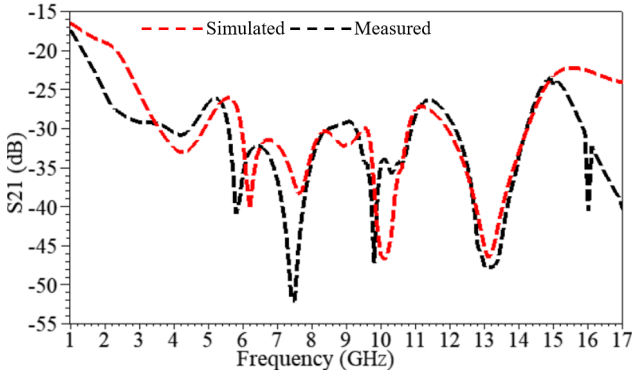

Figure 11. Comparison of S_{21} parameter of proposed MIMO antenna.

below −30 dB (at 6.0, 7.9, 9.6, and 12.7 GHz), below −20 dB at (11.1 and 15.6 GHz), and below −19 dB (at 2.2 GHz) frequency bands. From the above discussion, it is evident that the introduction of stubs in the ground plane helps in the improvement of isolation of proposed MIMO antenna along with the reflection coefficient and shifting the frequency band towards the lower side from 5.05 to 1.00 GHz.

The normalized 2D-radiation patterns in E-plane (XZ-plane) and H-plane (YZ-plane) of proposed MIMO antenna are delineated in Fig. 12 at unique resonance frequency points such as 2.2, 6.0, 7.9, 9.6, 11.1, 12.7, and 15.6 GHz. Fig. 12 also exemplifies the simulated and experimental cross-polarization and co-polarization radiation patterns for both the ports by exciting one port and terminating the other port by 50 Ω load impedance and vice versa. From Fig. 12, the radiation pattern is almost omnidirectional in both the planes at lower frequency and distorted at higher frequencies. Parallelly, it

can also be noted from the same figure that there are normalized patterns of co- and cross-polarizations which clearly indicate the isolation of almost more than 20 dB in XZ-plane and 15 dB in YZ-plane mainly in the main lobe direction (slightly varying around $\pm 90°$) at operational frequencies, which leads to the understanding that the antenna is linearly polarized. The pattern diversity of antenna has also got enhanced while it is moved from lower to higher resonant frequency in the XZ-plane for the entire operational frequency bands. The levels of co-polarization in XZ- and YZ-planes at the higher frequency bands are slightly distorted, and the cross-polarization level has increased due to the varied short wavelength electric current on the structure of proposed antenna. It can be contemplated from afore-said discussion that antenna propounds the directional properties which make it an efficient

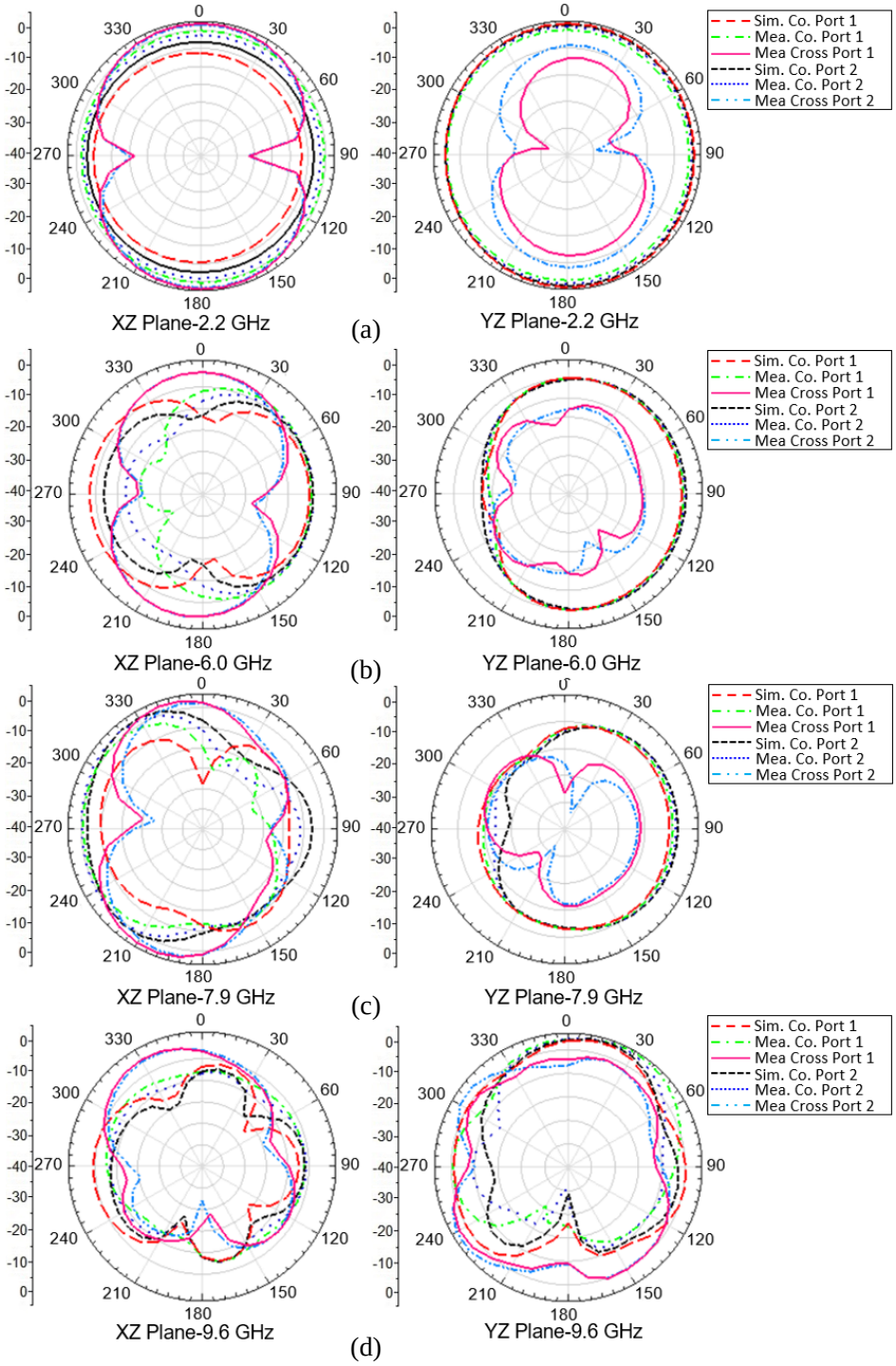

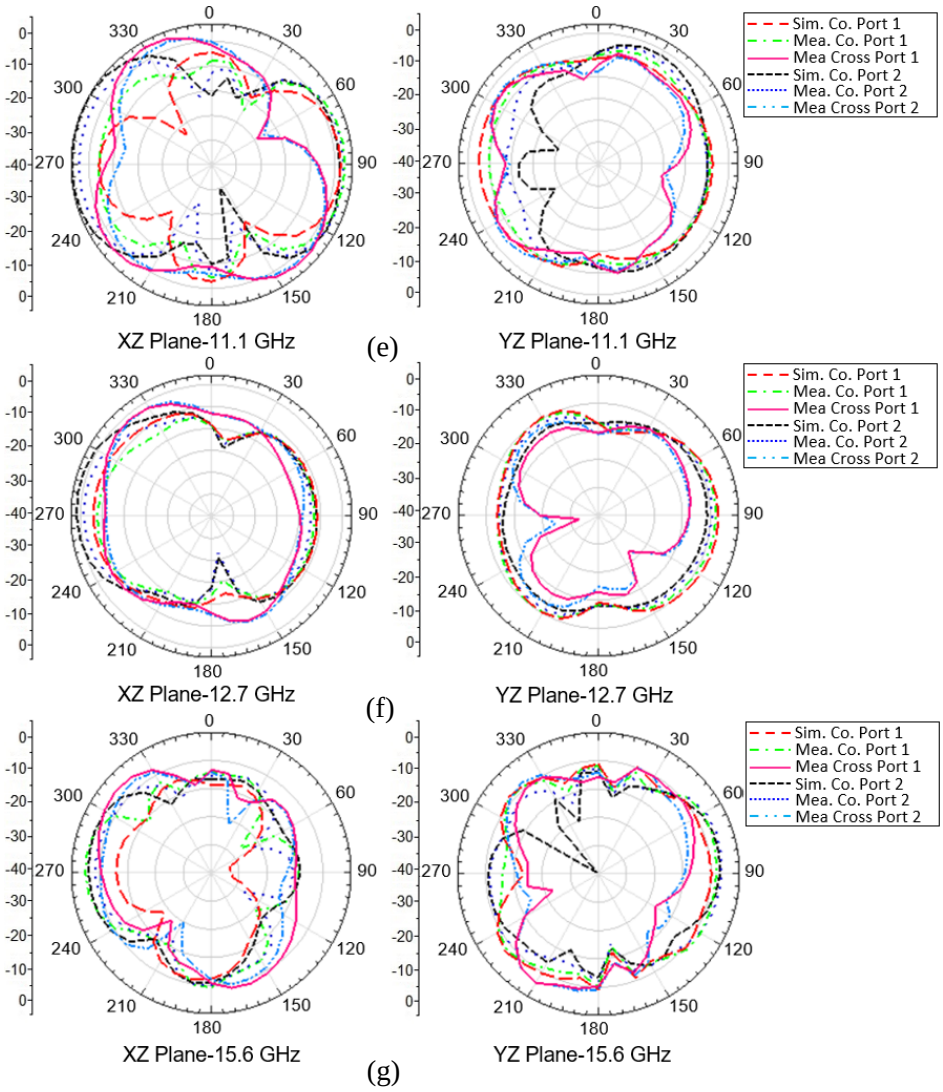

Figure 12. Normalized radiation patterns of proposed MIMO antenna at (a) 2.2, (b) 6.0, (c) 7.9, (d) 9.6, (e) 11.1, (f) 12.7 and (g) 15.6 GHz in both E (XZ-plane) and H (YZ-plane).

candidate for different wireless standards in the desired frequency range. The peak realized gains of proposed MIMO antenna are reported in Fig. 13. Proposed MIMO antenna's radiators are symmetrical in the structure; consequently, the simulated and measured gain values are almost identical. Therefore, the peak realized gain of single radiator is portrayed here. The simulated and fabricated antennas report the maximum gain of 8.86 dBi and 5.24 dBi, respectively. Proposed simulated and measured MIMO antennas also reveal the almost positive value of gain in the entire operating frequency range. The variation between the simulated and measured gains is noted which may have occurred due to the fabrication weaknesses such as connector soldering bumps, improper copper etching, some alterations in physical dimensions of the fabricated prototype, and environmental conditions.

4. DIVERSITY PARAMETERS OF PROPOSED MIMO ANTENNA

MIMO antenna's different diversity performance parameters like ECC (Envelope Correlation Coefficient), DG (Diversity Gain), CCL (Channel Capacity Loss), TARC (Total Active Reflection Coefficient) and MEG (Mean Effective Gain) are required to be analysed and evaluated for its efficient performance. These diversity parameters are studied and described in detail in the following subsections.

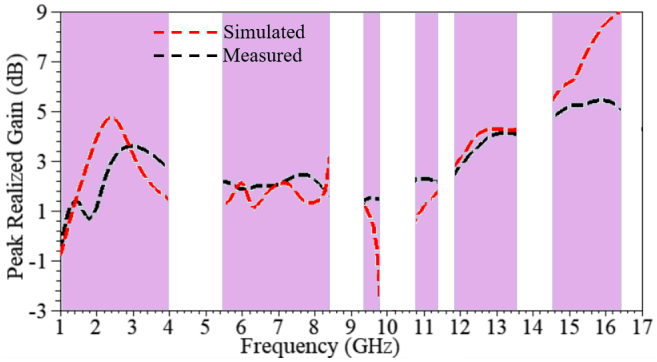

Figure 13. Peak realized gain versus frequency plot of proposed MIMO antenna.

4.1. ECC (Envelope Correlation Coefficient) and DG (Diversity Gain)

ECC is related to radiation pattern, and rather, it propounds how two antennas' radiation patterns are independent to each other. If one antenna is horizontally polarised, the other antenna will be vertically polarised, then the two antennas have zero correlation. Therefore, the correlation between radiation patterns of the two antennas can be termed as the ECC of MIMO antenna. Ideally, the required ECC value is zero, but practically it is not feasible, so acceptable limit of ECC is less than 0.5 (ECC < 0.5). The proposed MIMO antenna's ECC has been computed using S-parameters stated in the following equations. Simulated and experimental ECCs of the proposed MIMO antenna are shown in Fig. 14(a), and it is perceived that computed ECC values are within the acceptable limits for all the operational frequency bands [23, 24].

$$\text{ECC} = \frac{\left|S_{11}^{*}S_{12} + S_{21}^{*}S_{22}\right|^{2}}{\left(1 - \left(\left|S_{11}\right|^{2} + \left|S_{21}\right|^{2}\right)\right)\left(1 - \left(\left|S_{22}\right|^{2} + \left|S_{12}\right|^{2}\right)\right)} \tag{3}$$

Diversity gain (DG) can be said as the increase in signal-to-interference ratio because of diversity schemes, or it is the degree of effectiveness of diversity. The desired value of DG should be high or nearly 10 dB at operative frequency band, for attaining good quality and reliability in wireless systems. The DG of MIMO antenna is calculated from ECC by using Equation (4). The simulated and measured DGs are delineated in Fig. 14(b). From this figure, it can be substantiated that the DG of the proposed MIMO antenna at the operational frequency range is 10 dB (approximately) [25].

$$\text{DG} = 10 \times \sqrt{1 - |\text{ECC}|} \tag{4}$$

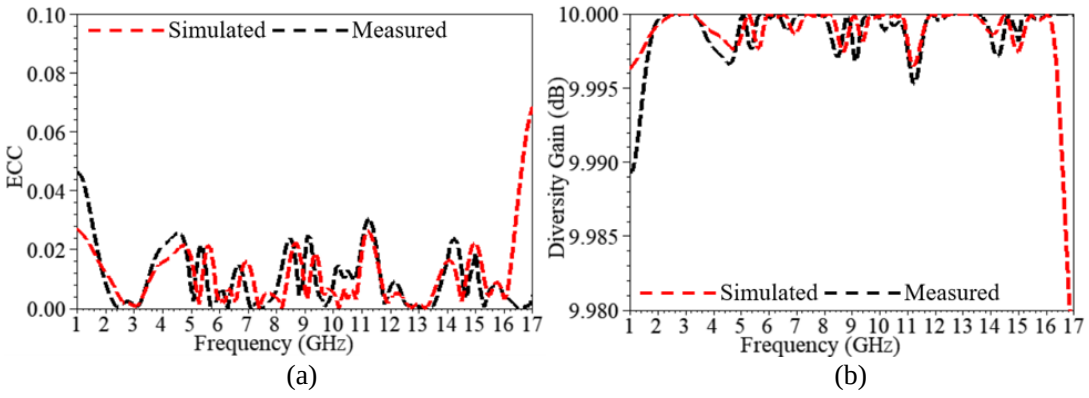

Figure 14. Simulated and measured comparison of (a) Envelope Correlation Coefficient (ECC) and (b) Diversity Gain (DG) of proposed MIMO antenna.

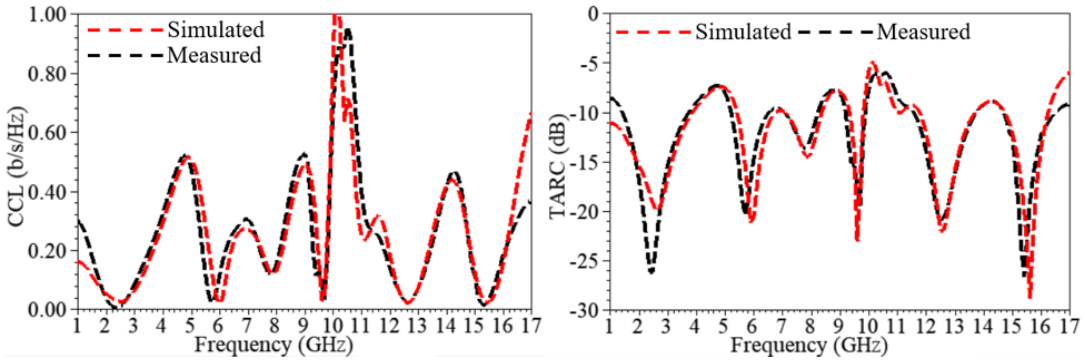

Figure 15. Simulated and measured comparison of (a) Channel Capacity Loss (CCL) and (b) Total Active Reflection Coefficient (TARC) of proposed MIMO antenna.

4.2. CCL (Channel Capacity Loss) and TARC (Total Active Reflection Coefficient)

The CCL of MIMO antenna is the maximum consistent data transmission rate without any loss in the communication channel. The CCL's ideal accepted minimum value is less than 0.4 bits/sec/Hz. The comparison of simulated and measured CCL versus frequency plots of the proposed MIMO antenna is illustrated in Fig. 15(a). CCL can be computed using Equations (5) to (6). It can be corroborated that the value of CCL is much below the desired maximum value (< 0.4 bits/sec/Hz) at the required operative frequencies [26].

$$C_{\text{loss}} = -\log_2 \left|\beta^R\right| \tag{5}$$

$$\beta^R = \begin{bmatrix} \beta_{11} & \beta_{12} \\ \beta_{21} & \beta_{22} \end{bmatrix} \tag{6}$$

where,

$$\begin{aligned} \beta_{11} &= 1 - \left(|S_{11}|^2 + |S_{12}|^2\right) \\ \beta_{22} &= 1 - \left(|S_{22}|^2 + |S_{21}|^2\right) \\ \beta_{12} &= -\left(S_{11}^* S_{12} + S_{21}^* S_{22}\right) \\ \beta_{21} &= -\left(S_{22}^* S_{21} + S_{12}^* S_{11}\right) \end{aligned}$$

For N-port antenna, TARC parameter is related to the total incident power and total outgoing power. Ideally, it should be zero which means that the complete power delivered shall be accepted by the antenna. Therefore, it is defined as the ratio of the square root of the total reflected power by the square root of total incident power [26]. The generalized TARC for N port antenna and for the case of 2 port antenna can be computed from Equations (7) and (8). The comparison of simulated and measured TARCs of proposed MIMO antenna is envisaged in Fig. 15(b).

$$\Gamma_a^t = \frac{\sqrt{\sum_{i=1}^{N} |b_i|^2}}{\sqrt{\sum_{i=1}^{N} |a_i|^2}} \tag{7}$$

$$\Gamma_a^t = \frac{\sqrt{\left(\left|\left(S_{11} + S_{12}^{e^{j\theta}}\right)\right|^2 + \left|\left(S_{21} + S_{22}^{e^{j\theta}}\right)\right|^2\right)}}{\sqrt{2}} \tag{8}$$

where,

$b_i = [S] \cdot a_i \cdot [S]$ is the scattering matrix

$[b] \rightarrow$ scattering vector and $[a] \rightarrow$ excitation vector

4.3. MEG (Mean Effective Gain)

MEG of MIMO antenna is defined as the ratio of the mean received power to the mean incident power, and its ideal value shall lie within the specified limit of ±3 dB. The ration of MEG should abide the criteria $|\mathrm{MEG}_i/\mathrm{MEG}_j| < \pm 3\,\mathrm{dB}$ for attaining better diversity performance, where i and j indicate antenna elements 1 and 2, respectively [27]. Proposed MIMO antenna's MEG is calculated from Equations (9) to (10), and the promising result is delineated in Fig. 16.

$$\mathrm{MEG}_i = 0.5\left[1 - |S_{ii}|^2 - |S_{ij}|^2\right] \tag{9}$$

$$\mathrm{MEG}_j = 0.5\left[1 - |S_{ij}|^2 - |S_{jj}|^2\right] \tag{10}$$

The proposed MIMO antenna has been designed and investigated for distinct wireless applications. Although there are several MIMO antennas in existing literature, the proposed MIMO antenna is highly competitive compared to the reported designs in terms of size, isolation, and overall operational frequency band coverage. The proposed antenna is compact in size and also reveals efficient performance. The comprehensive parametric comparison of designed antenna with the available state-of-art literature is tabulated in Table 3 for more limpidity. Thus, it can be anticipated from the table that ECC, CCL, and TARC of the proposed MIMO antenna are at the desirable values, whereas most of the reported designs are not evaluated in terms of TARC and CCL. From the afore-mentioned discussion, it is quite evident that the proposed antenna can be used for multi-standard wireless applications such as 1800 MHz 2G spectrum of GSM band (1.71–1.88 GHz), Aircraft Surveillance (1.09 GHz), 3G Cellular Communication Mobile Uplink (1.90–1.98 GHz), Advance Wireless Services (2.11–2.15 GHz), LTE 2300/LTE 2500 (2.3–2.4 GHz/2.5–2.69 GHz), RFID (2.4 GHz/5.4 GHz), Wi-Fi (2.4–2.485 GHz), Bluetooth (2.4 GHz),

Table 3. Comparison of proposed MIMO antenna with existing literature.

Reference	Band coverage	Dimension ($\mathbf{mm^2}$)	Isolation (dB)	ECC	TARC	CCL	Ports
[6]	Two	11250	15	< 0.02	—	—	4
[7]	Two	3600	< 20	< 0.08	—	—	2
[8]	Three	2500	20–50	< 0.01	-10	—	4
[28]	Three	6000	20–40	< 0.04	—	—	2
[29]	Two	7200	30	—	—	—	2
[30]	Two	2552	35	0.007	—	—	2
[31]	Three	60000	25	0.001	—	—	2
[32]	Two	5640	20	< 0.04	—	—	2
[33]	One	5000	20–40	0.0007	—	—	2
[34]	Four	6000	< 30	—	—	—	2
[35]	Two	7484.61	< 20	< 0.1	—	—	2
[36]	Four	9600	> 15	< 0.5	—	—	2
[37]	Four	9600	< 15	< 0.5	—	—	2
[38]	Four	7800	< 20	< 0.5	—	—	2
[39]	Five	3500	< 30	< 0.028	-8	< 0.3	2
This work	Seven	1560	20–40	< 0.024	-9.96	< 0.23	2

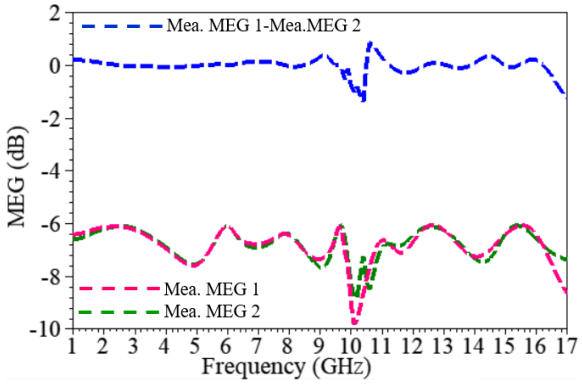

Figure 16. Mean Effective Gain (MEG) of proposed MIMO antenna between port (1, 2).

WLAN (2.4–2.484 GHz/5.15–5.35 GHz/5.72–5.825 GHz), Wi-MAX (3.2–3.85 GHz), C-band downlink-uplink (3.72–4.2 GHz/5.925–6.425 GHz), 5G spectrum band (5900–6400 MHz) adopted by European Union, broadcasting satellites (12.4–12.5 GHz), FSS (11.45–11.7/12.5–12.75 GHz), and defense systems (14.62–15.23 GHz).

5. CONCLUSION

A compact size modified spokes wheel shaped two port MIMO antenna with stub loaded ground plane has been expounded in this manuscript for multiband wireless applications. The proposed MIMO antenna is investigated by using two distinct types of ground plane (ground-1 and ground-2). Performance of the proposed antenna with different ground planes has been compared, and it is found that the antenna with ground-2 is better in terms of increase in number of frequency bands, improved bandwidth, reflection coefficient, and reduction in mutual coupling. Proposed MIMO antenna exhibits seven frequency bands with improved isolation ($S_{12/21}$) −19.47, −31.22, −34.63, −30.05, −27.16, −39.08, and −22.28 dB. The Envelope Correlation Coefficient (ECC) and Channel Capacity Loss (CCL) are less than 0.03 and 0.3 bits/sec/Hz for the operational bandwidth of desired resonant frequency band. Other diversity performance parameters such as DG, MEG, and TARC are also found in suitable limits. Proposed antenna is useful for different multi-standard wireless applications because of acceptable limits of afore-said performance parameters.

REFERENCES

1. Chung, H., Y. Jang, and J. Choi, "Design of a multiband internal antenna for mobile application," *Proceed. of the IEEE Int. Sympo. Ant. Propag. & USNC/URSI National Radio Sci. Meeting*, 1–4, 2009.
2. Sehrai, D.-A., M. Abdullah, A. Altaf, S.-H. Kiani, F. Muhammad, M. Tufail, M. Irfan, A. Glowacz, and S. Rahman, "A novel high gain wideband MIMO antenna for 5G millimeter wave applications," *Electronics*, Vol. 9, No. 1031, 1–13, 2020.
3. Yang, Y.-Y., Q. Chu, and C. Mao, "Multiband MIMO antenna for GSM, DCS, and LTE indoor applications," *IEEE Ant. Wirel. Propag. Lett.*, Vol. 16, 1573–1576, 2016.
4. Hatte, J.-S. and R.-B. Patil, "Design methods of MIMO antenna for 5G new radio applications in mobile terminals — A review," *Int. J. Emerg. Technol.*, Vol. 11, No. 3, 738–745, 2020.
5. Nandi, S. and A. Mohan, "A compact dual-band MIMO slot antenna for WLAN applications," *IEEE Ant. Wirel. Propag. Lett.*, Vol. 16, 2457–2460, 2017.
6. Huang, J., G. Dong, Q. Cai, Z. Chen, L. Li, and G. Liu, "Dual-band MIMO antenna for 5G/WLAN mobile terminals," *Micromachines*, Vol. 12, No. 489, 1–12, 2021.

7. Deng, J.-Y., Z.-J. Wang, J.-Y. Li, and L.-X. Guo, "A dual-band MIMO antenna decoupled by a meandering line resonator for WLAN applications," *Microw. Opt. Technol. Lett.*, Vol. 60, 759–765, 2018.
8. Kumar, A., S.-K. Mahto, R. Sinha, and A. Choubey, "Dual circular slot ring triple-band MIMO antenna for 5G applications," *Frequenz*, Vol. 75, Nos. 3–4, 91–100, 2021.
9. Liu, Y., Y. Lin, Y. Liu, J. Ren, J. Wang, and X. Li, "Dual-band planar MIMO antenna for WLAN application," *Microw. Opt. Technol. Lett.*, Vol. 57, 2257–2262, 2015.
10. Ishteyaq, I. and K. Muzaffar, "Multiple input multiple output (MIMO) and fifth generation (5G): And indispensable technology for sub-6 GHz and millimeter wave future generation mobile terminal applications," *Int. J. Microw. Wirel. Technol.*, 1–17, 2021.
11. Talha, M.-Y., K.-J. Babu, and R.-W. Aldhaheri, "Design of a compact MIMO antenna system with reduced mutual coupling," *Int. J. Microw. Wirel. Technol.*, Vol. 8, No. 1, 117–124, 2016.
12. Wang, F., Z. Duan, X. Wang, Q. Zhou, and Y. Gong, "High isolation millimeter-wave wideband MIMO antenna for 5G communication," *Int. J. Ant. Propag.*, Vol. 4283010, 1–12, 2019.
13. Nirmal, P. C., A. Nandgaonkar, S. L. Nalbalwar, and R. K. Gupta, "A compact dual band MIMO antenna with improved isolation for Wi-MAX and WLAN applications," *Progress In Electromagnetics Research M*, Vol. 68, 69–77, 2018.
14. Iqbal, A., O.-A. Saraereh, and A.-W. Ahmad, "Mutual coupling reduction using F-shaped stubs," *IEEE Access*, Vol. 6, 2755–2759, 2017.
15. Sun, J.-S., H.-S. Fang, and P.-Y. Lin, "Triple-band MIMO antenna for mobile wireless applications," *IEEE Ant. Wirel. Propag. Lett.*, Vol. 15, 500–503, 2016.
16. Asadpor, L. and M. Rezvani, "Multiband microstrip MIMO antenna with CSRR loaded for GSM and LTE applications," *Microw. Opt. Technol. Lett.*, Vol. 60, No. 12, 3076–3080, 2018.
17. Deng, J., J. Li, L. Zhao, and L. Guo, "A dual-band inverted-F MIMO antenna with enhanced isolation for WLAN applications," *IEEE Ant. Wirel. Propag. Lett.*, Vol. 16, 2270–2273, 2017.
18. Dong, J., X. Yu, and L. Deng, "A decoupled multiband dual-antenna system for WWAN/LTE smartphone applications," *IEEE Ant. Wirel. Propag. Lett.*, Vol. 16, 1528–1532, 2017.
19. Khan, A.-A., M.-H. Jamaluddin, S. Aqeel, J. Nasir, J.-R. Kazim, and O. Owais, "Dual-band MIMO dielectric resonator antenna for WiMAX/WLAN applications," *IET Microw. Ant. Propag.*, Vol. 11, No. 1, 113–120, 2017.
20. Wang, H., R. Zhang, Y. Luo, and G. Yang, "Design of MIMO antenna system operating in wideband of 3300 to 6400 MHz for future 5G mobile terminal applications," *Int. J. RF Microw. Comput. Aided Eng.*, Vol. 30, No. 10, 1–21, 2020.
21. Sharma, N. and S.-S. Bhatia, "Metamaterial inspired fidget spinner shaped antenna based on parasitic split ring resonator for multi standard wireless applications," *Journal of Electromagnetic Waves and Applications*, Vol. 34, No. 10, 1471–1490, 2019.
22. Sharma, N. and S. S. Bhatia, "Stubs and slits loaded partial ground plane inspired novel hexagonal ring-shaped fractal antenna for 5G/LTE/RFID/GSM/Bluetooth/WLAN/WiMAX wireless applications: Design and measurement," *Progress In Electromagnetics Research C*, Vol. 112, 99–111, 2021.
23. Babu, K.-V. and B. Anuradha, "Design of multi-band Minkowski MIMO antenna to reduce the mutual coupling," *J. King Saud. Uni.-Eng. Sci.*, Vol. 32, No. 1, 51–57, 2018.
24. Dkiouak, A., A. Zakriti, M. El Ouahabi, H. Elftouh, and A. Mchbal, "Design of CPW-fed MIMO for ultra-wideband communications," *Procedia Manuf.*, Vol. 46, 782–787, 2020.
25. Gurjar, R., D.-K. Upadhyay, B.-K. Kanaujia, and A. Kumar, "A compact modified Sierpinski carpet fractal UWB MIMO antenna with square-shaped funnel like ground stub," *AEU-Int. J. Electron. Commun.*, Vol. 117, 153126, 2020.
26. Saadh, A. W. M., K. Ashwath, and P. Ramaswamy, "A uniquely shaped MIMO antenna on FR4 material to enhance isolation and bandwidth for wireless applications," *AEU-Int. J. Electron. Commun.*, Vol. 123, 153316, 2020.

27. Gurjar, R., D. K. Upadhyay, B. Kanaujia, and A. Kumar, "A compact U-shaped UWB-MIMO antenna with novel complementary modified Minkowski fractal for isolation enhancement," *Progress In Electromagnetics Research C*, Vol. 107, 81–96, 2021.
28. Roy, S. and U. Chakraborthy, "Mutual coupling reduction in a multi-band MIMO antenna using meta-inspired decoupling network," *Wirel. Person Commun.*, Vol. 114, 3231–3246, 2020.
29. Pan, C. and T.-J. Cui, "Broadband decoupling network for dual-band microstrip patch antennas," *IEEE Trans. Ant. Propag.*, Vol. 65, No. 10, 5595–5598, 2017.
30. Tan, X., W. Wang, Y. Wu, Y. Liu, and A.-A. Kishk, "Enhancing isolation in dual-band Meander-line multiple antennas by employing split EBG structure," *IEEE Trans. Ant. Propag.*, Vol. 67, No. 4, 2769–2774, 2019.
31. Jiang, Z.-H., "A compact triple-band antenna with a notched ultra-wideband and its MIMO array," *IEEE Trans. Ant. Propag.*, Vol. 66, No. 12, 7021–7031, 2018.
32. Liu, X., Y. Wu, Z. Zhuang, W. Wang, and Y. Liu, "A dual-band patch antenna for pattern diversity application," *IEEE Access*, Vol. 6, 51986–51993, 2018.
33. Zhao, X., S.-P. Yeo, and L.-C. Ong, "Decoupling of inverted-F antennas with high-order modes of ground plane for 5G mobile MIMO platform," *IEEE Trans. Ant. Propag.*, Vol. 66, No. 9, 4485–4495, 2018.
34. Yang, Y., Q. Chu, and C. Mao, "Multiband MIMO antenna for GSM, DCS, and LTE indoor applications," *IEEE Ant. Wirel. Propag. Lett.*, Vol. 15, 1573–1576, 2016.
35. Peristerianos, A., A. Theopoulos, A.-G. Koutinos, T. Kaifas, and K. Siakavara, "Dual-band fractal semi-printed element antenna arrays for MIMO applications," *IEEE Ant. Wirel. Propag. Lett.*, Vol. 15, 730–733, 2016.
36. Wang, S. and Z. Du, "A multiband dual-antenna system with a folded fork-shaped ground branch and folded asymmetric U-shaped slots for smartphone applications," *IEEE Ant. Wirel. Propag. Lett.*, Vol. 14, 1626–1629, 2015.
37. Wang, S. and Z. Du, "Decoupled dual-antenna system using crossed neutralization lines for LTE/WWAN smartphone applications," *IEEE Ant. Wirel. Propag. Lett.*, Vol. 14, 523–526, 2015.
38. Hussain, R. and M.-S. Sharawi, "Integrated reconfigurable multiple input–multiple-output antenna system with an ultra-wideband sensing antenna for cognitive radio platforms," *IET Microw. Ant. Propag.*, Vol. 9, No. 9, 940–947, 2015.
39. Saleem, R., M. Bilal, H.-T. Chattha, S.-U. Rehman, A. Mushtaq, and M.-F. Shafique, "An FSS based multiband MIMO system incorporating 3D antennas for WLAN/WiMAX/5G cellular and 5G Wi-Fi applications," *IEEE Access*, Vol. 7, 144732–144740, 2019.